

Tire Test for Drifting Dynamics of a Scaled Vehicle

Ronnapee C* and Witaya W

Department of Mechanical Engineering, Faculty of Engineering, Chulalongkorn University
Wang Mai, Patumwan, Bangkok, 10330

Abstract

Drifting is a cornering technique with large angle of sideslip. In some special conditions, however more advantageous it is, drifting is high risk to loss of control. Due to difficulties and perils of drifting, the study of drifting dynamic on scaled vehicle test is more preferable. Because of the large amount of tire slip while drifting, tire forces cannot be linearly estimated with the tire cornering stiffness. In this study, scaled vehicle's tire forces occurring at high slip condition were studied by means of a drum tire test. The drum tire tester was designed and developed to control the slip conditions, consisting of slip angle and slip ratio, and to measure the tire friction forces consistent with each slip condition. While testing, the slip angle was determined by the steering angle of the tested wheel and the slip ratio was controlled by the rotational speeds of drum and the wheel. Despite small unbalances of drum and wheel, vertical load was controlled by the use of counter weight. The tire friction forces, both lateral and longitudinal, were measured by the ATI Gamma force sensor. Eventually, the experimental data was used to fit parameters of Magic Formula tire friction model. The obtainable tire friction model can be applied to estimate the tire forces of scaled vehicle at high slip drifting condition.

Keywords: Scaled vehicle, Magic formula, Tire friction model, Drum tire tester, Slip condition

1. Introduction

Drifting is a cornering technique with large angle of sideslip. As it can be frequently seen in dirt rally and driving on snow or wet road or even in memorable scene of racing films, drifting seems to be more advantageous in some special conditions. Likewise, the simulation results of steady state drifting [2] which show that drifting provides the higher cornering velocity than conventional driving while radius of curvature greater than the specific radius. In the research, a two dimensional dynamics model, namely the Bicycle model, was constructed with a nonlinear tire model, the semi-empirical combined-slip Pacejka Magic Formula [9], to represent planar drifting of RWD car in steady state when radius of curvature, absolute velocity and side slip are constant.

However, drifting is not a natural thing for a normal driver. In fact, this technique requires special skills of driver to turn cornering with large amplitude of sideslip. Furthermore, the vehicle is high risk to loss of control while drifting. Consequently, a driver has to control the suitable slip of each four tires to sustain the equilibrium of forces and moments [1] so that the vehicle aligns in the desired direction and travels along the desired path. Due to difficulties and perils of drifting on full size car, the study of drifting dynamic on scaled vehicle test is more preferable.

Nowadays, the study in dynamics behavior of real vehicle's by experimenting on scaled vehicle becomes more popular. In [4], the 1:10 scaled model car was modified to comply with the Similarity law to be the test vehicle. In [5], the 3D dynamic model of scaled vehicle was constructed with linear tire model, obtained from the test of 1:10 scaled tire with the developed drum tire tester. In this study, only lateral tire force was measured at small slip angle so that the tire cornering stiffness could be determined. The derived 3D dynamics model was used for Interactive Dynamic Simulation with scaled vehicle from [4]. In [6], the scaled model testing apparatus, consisting of vehicle and treadmill, was developed so that the dynamics of vehicle at low slip condition could be study. Besides, the cornering stiffness testing apparatus was modified of the same treadmill. The apparatus had important features similarly with the

tire test in [5]. The only different is that the treadmill was used in [6] whereas drum was used in [5]. Finally, both of these tire test apparatuses could not control the slip ratio.

Dynamics characteristics of a scaled vehicle can be applied to describe a large number of real situations by means of Similarity Law.

Experiments using scaled vehicle test have advantages over real vehicle test in many ways. First of all, testing condition is safer. Moreover, experimental setting up is much cheaper; small testing area is sufficient for experiment. Besides, the positioning measurement in scaled environment can be easily implemented by a vision system or other techniques which provide better accuracy than GPS measurement in a real track.

Tire friction, the crucial factor affecting on dynamic of a vehicle, consists of two components: lateral force and longitudinal force. Magnitudes of both components relative to vertical load and current slip condition, consisting of lateral slip, measured in terms of slip angle and longitudinal slip, measured in terms of slip ratio. While drifting, the combined slip occurs at rear tire; furthermore, magnitudes of both slip ratio and slip angle are so high that the tire frictions cannot be estimated by linear function. The Pacejka Magic Formula [7], the renowned tire friction model used in both educational and industrial purpose, is necessary for this study. Therefore, all parameters of Magic Formula must be fitted with experimental data.

Drum tire test is one of the most renowned methods for both full-sized and scaled tire. As previously mentioned that the drum tire tester for scaled tire in [5, 6] was not designed for non-zero slip ratio test. Therefore, it is imperative that the drum tire tester be designed and constructed.

2. Pacejka Magic Formula

In this section, the two general form of Pacejka Magic Formula will be described.

2.1 The Sine form of Magic formula

The general form of Sine relation is shown in Fig. 1.

* Corresponding Author: E-mail: kkpreech@kmitl.ac.th, Tel: 02 329 8261-2, Fax: 02 737 2580,

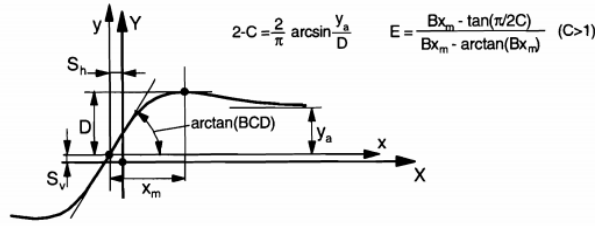


Fig.1 General Form of Sine Relation

The Sine relation is commonly used to describe the relation between lateral force and slip angle as Eq. (1) or the relation between longitudinal force and slip ratio as Eq. (2).

$$F_y = D \sin[\text{Carctan}[B\alpha - E(B\alpha - \arctan B\alpha)]] \quad (1)$$

$$F_x = D \sin[\text{Carctan}[Bk - E(Bk - \arctan Bk)]] \quad (2)$$

When B is Stiffness factor
 C is Shape factor
 D is Peak factor
 E is Curvature factor

2.2 The Cosine form of Magic formula

The general form of Cosine relation is shown in Fig. 2.

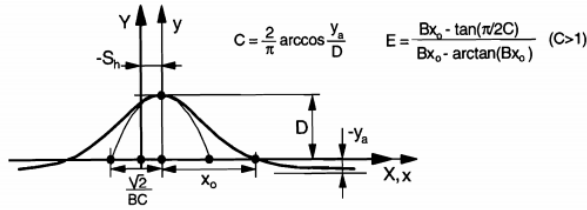


Fig.2 General Form of Cosine Relation

The Cosine relation is commonly used to describe the relation between lateral force and slip ratio as Eq. (3) or the relation between longitudinal force and slip angle as Eq. (4).

$$F_y = D \cos[\text{Carctan}[Bk]] \quad (3)$$

$$F_x = D \cos[\text{Carctan}[B\alpha]] \quad (4)$$

When B is Stiffness factor
 C is Shape factor
 D is Peak factor
 E is Curvature factor

3. Drum Tire Tester for 1:10th Scaled Tire

The desired tire tester must be able to control slip conditions and to measure the magnitudes of tire forces in both two components instantly. Furthermore, the whole system must be able to slide in the vertical direction in order that the effects of unbalance due to the drum and the wheel can be compensated.

3.1 Conceptual design

The conceptual design of the drum tire tester is illustrated in Fig. 3. In this design, a counter weight, connected with whole system by a cable wrapping around a pulley, was used to balance the mass of whole system; a pair of linear bearing was also used to guide the vertical movement of the whole system due to unbalances of the drum and the tested wheel. The 20 cm diameter drum, driven by DC motor, was used to simulate linear velocity of road relating to center of the tested wheel. Moreover, the other smaller DC motor was used to drive the tested wheel directly so that the desired longitudinal slip between road and tire contact patch could be generated. The screw mechanism was used to fix desired position of the adjustable steering wheel module. Beside, rotary encoder was installed to measure slip angle, equal to steering angle. Finally, force sensor was installed above steering wheel set so that magnitudes of tire force in both components can be measured instantly.

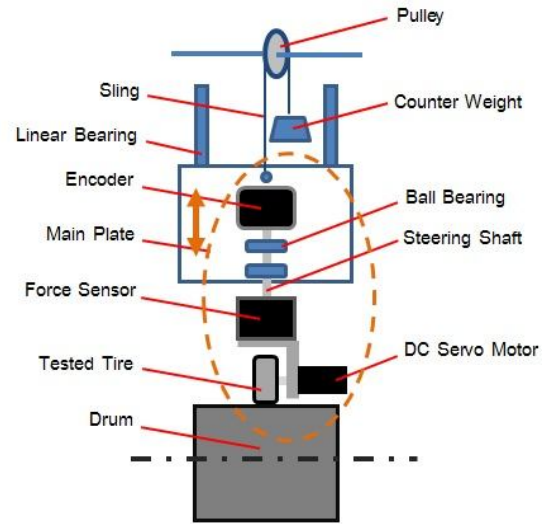


Fig. 3 Conceptual design

In order to develop the actual system, CAD was used to design manufactured parts. The detail design of whole system by CATIA is shown in Fig. 4. In this figure, important modules and their positions are illustrated.

3.2 Actual system

Manufactured parts were assembled together with a pair of linear bearings, DC driver motor, tested wheel and measuring instruments; ATI gamma force/torque sensor and Electronic GmbH D78647 rotary encoder. The whole system was mounted with existing frame base as illustrated in Fig. 5 below.

The steering wheel module, consisting of tested wheel, DC driver motor and ATI gamma force/torque sensor, is shown in the left of Fig. 6. The position of the counter weight is shown in the right of Fig. 6. The Electronic GmbH D78647 10000 PPR rotary encoder was installed and connected with Sensoray 626 DAQ card so that steering angle was displayed on MATLAB Simulink real-time workshop as shown in the same figure.

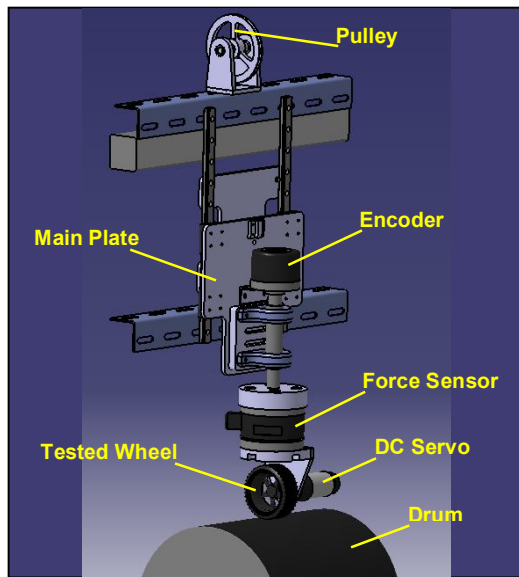


Fig. 4 Detail design by CATIA

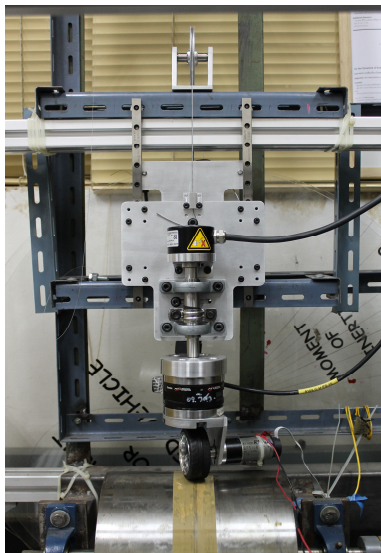


Fig. 5 Tire testing system

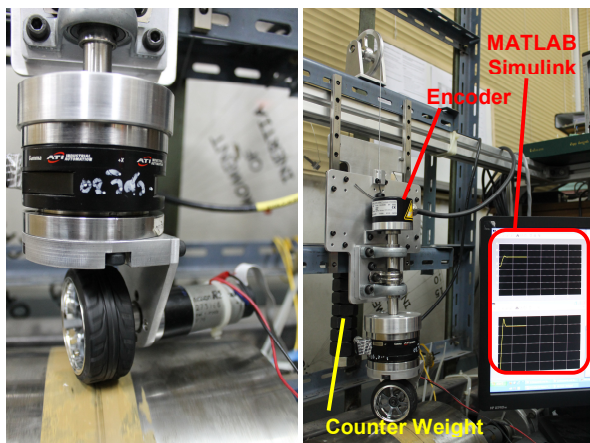


Fig. 6 Steering wheel module (Left) Counter weight & Encoder (Right)

4. Tire Testing Procedure

The relations between tire friction forces and varied slip conditions were studied by the experimenting on the 1:10th scaled HPI T-Grip commercial tires. The ATI Gamma force/torque sensor was used to measure tire forces meanwhile their real-time value were appeared on screen by the application of ATI DAQ F/T demo software. The testing procedure will be described in this section.

In the beginning, the relation between lateral force and slip angle was studied by means of pure lateral slip test, where longitudinal slip was zero. During the test, the DC motor driving tested wheel was not active; the tested wheel was only driven by the spinning drum. On the other hand, the slip angle was adjusted from 0 to 90 degrees. For every slip angle, the measured lateral forces were manually recorded into text file while vertical load was in desired ranges: 2.3 - 2.7 N, 3.3 - 3.7 N and 4.3 - 4.7 N, which represent 2.5 N, 3.5 N and 4.5 N of vertical loads respectively.

Subsequently, longitudinal force and lateral force, varying with slip ratio, were studied. The slip angle was fixed to be constant at 20 degrees. On the other hand, by controlling speed of the drum and the tested wheel, slip ratio could be adjusted over desired range from 0 to 1. The measured lateral and longitudinal forces were recorded while vertical load was in desired range: 3.3 - 3.7 N, representing 3.5 N of vertical load.

Finally, the relation between longitudinal force and slip angle was studied. The slip ratio was controlled to be constant at 0.1 whereas the slip angle was adjusted from 0 to 90 degrees. The measured longitudinal forces were recorded while vertical load was in desired range: 3.3 - 3.7 N, which represent 3.5 N of vertical load.

5. Tire Testing Results

Tire friction forces both lateral and longitudinal, corresponding to varied slip conditions, will be described in this section. In the relationship plot below, experimental raw data (Exp) will be represented by blue squares. Besides, average values (Avg) and Magic formula estimated values (Magic) will be represented by green squares and red squares respectively.

5.1 The relation between lateral force and slip angle

According to the pure lateral slip testing results at 3.5N vertical load and zero slip ratio, the relationship plot between lateral force and slip angle is shown in Fig. 7, where horizontal axis is slip angle measured in degrees and vertical axis is lateral force measured in Newton. In this relation, Magic formula tire model derived from parameter fitting is shown in Eq. (5)

$$F_y = 6.5 \sin[1.58 \arctan[0.028\alpha - 1.62(0.028\alpha - \arctan(0.028\alpha))]] \quad (5)$$

Consider the plot of average values and Magic formula estimated values in Fig. 7, the lateral force increase linearly with increasing slip angle when slip angle is less than 20 degrees. Subsequently, lateral force still increase until reach maximum value at 40 degrees slip angle. Whereupon, the lateral force slightly decrease until the slip angle reaches 90 degrees.

Consider the plot of experimental raw data, at low slip angle, the width of uncertainty band increase with

increasing slip angle. Eventually, the widest uncertainty band occurs at about 40 degrees of slip angle. After that, the width seems to be constant until the slip angle reaches 90 degrees.

5.2 The relation between longitudinal force and slip ratio

According to the combined slip testing results at 3.5N vertical load and 20 degrees slip angle, the relationship plot between longitudinal force and slip ratio is shown in Fig. 8, where horizontal axis is slip ratio, dimensionless quantity, and vertical axis is longitudinal force measured in Newton. In this relation, Magic formula tire model derived from parameter fitting is shown in Eq. (6)

$$F_x = 5.5 \sin[1.27 \arctan[2.86k - 0.62(2.86k - \arctan(2.86k))]] \quad (6)$$

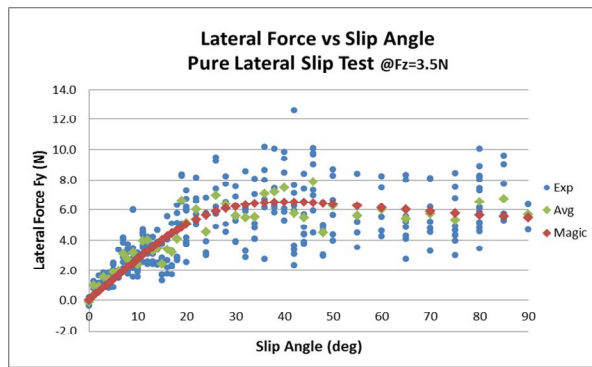


Fig. 7 Plot of Lateral force vs Slip angle in pure lateral slip test, at 3.5N vertical load

Consider the plot of average values and Magic formula estimated values in Fig. 8, the longitudinal force increase linearly with increasing slip ratio when slip ratio is less than 0.2. Subsequently, longitudinal force still increase until reach maximum value at slip ratio 0.3. Whereupon, the longitudinal force slightly decrease until the slip ratio reaches 1.

Consider the plot of experimental raw data, at low slip ratio, the width of uncertainty band increase with increasing slip ratio. Eventually, the widest uncertainty band occurs at slip ratio about 0.3. After that, the width of uncertainty band slightly decreases at larger slip ratio.

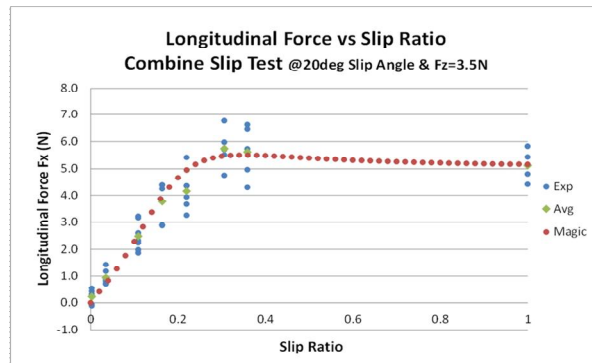


Fig. 8 Plot of Longitudinal force vs Slip ratio in combined slip test, at 3.5N vertical load

5.3 The relation between lateral force and slip ratio

According to the combined slip testing results at 3.5N vertical load and 20 degrees slip angle, the relationship plot between lateral force and slip ratio is shown in Fig. 9, where horizontal axis is slip ratio, dimensionless quantity, and vertical axis is lateral force measured in Newton. In this relation, Magic formula tire model derived from parameter fitting is shown in Eq. (7)

$$F_y = 8 \cos[1.33 \arctan(2.12k)] \quad (7)$$

Consider the plot of average values and Magic formula estimated values in Fig. 9, the maximum lateral force occurs at zero slip ratio. Subsequently, the value of lateral force decreases with increasing slip ratio. Eventually, the value is nearly zero when slip ratio reaches 1.

Consider the plot of experimental raw data, the uncertainty band is widest at zero slip ratio. Consequently, the width decrease with increasing slip ratio.

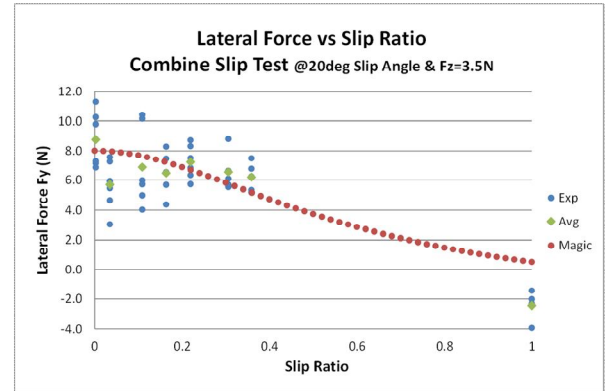


Fig. 9 Plot of Lateral force vs Slip ratio in combined slip test, at 3.5N vertical load

5.4 The relation between longitudinal force and slip angle

According to the combined slip testing results at 3.5N vertical load and slip ratio 0.1, the relationship plot between longitudinal force and slip angle is shown in Fig. 10, where horizontal axis is slip angle measured in degrees and vertical axis is longitudinal force measured in Newton. In this relation, Magic formula tire model derived from parameter fitting is shown in Eq. (8)

$$F_x = 3.6 \cos[1.18 \arctan(0.04\alpha)] \quad (8)$$

Consider the plot of average values and Magic formula estimated values in Fig. 10, the maximum longitudinal force occurs at zero slip angle. Subsequently, the value of longitudinal force decreases with increasing slip angle. Eventually, the value is nearly zero when slip angle reaches 90 degrees.

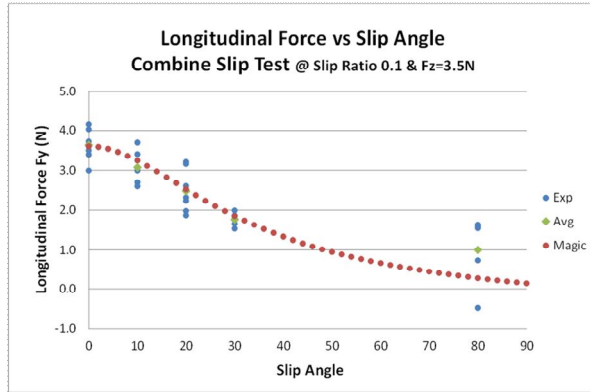


Fig. 10 Plot of Longitudinal force vs Slip angle in combined slip test, at 3.5N vertical load

5.5 The relation between lateral force and vertical load

The effect of vertical load on lateral force can be described by the experimental results in Fig. 11, showing the relation between slip angle and lateral force while vertical loads were 2.5N, 3.5N and 4.5N respectively. In conclusion, tire can generate larger amplitude of lateral force when it supports higher value of vertical load. Furthermore, the slip angle where maximum lateral force appears was slightly lower.

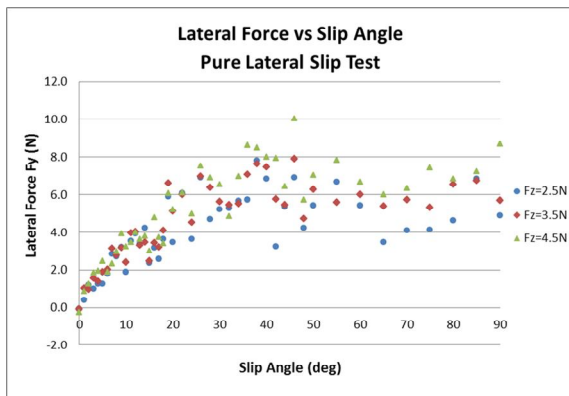


Fig. 11 Plot of Lateral force vs Slip angle in pure lateral slip test, varying vertical load

5.6 Magic formula estimating results for lateral and longitudinal forces

Consider four derived Magic formula estimating equations in the previous sections. Both Eqs. (3) and Eqs. (5) describe magnitude of lateral force, relating with slip angle and slip ratio respectively. The result of this estimation is shown in Fig. 12, where horizontal plane represents slip condition both slip angle and slip ratio. Besides, the vertical axis is longitudinal force measured in Newton.

Lateral Force vs Slip Condition

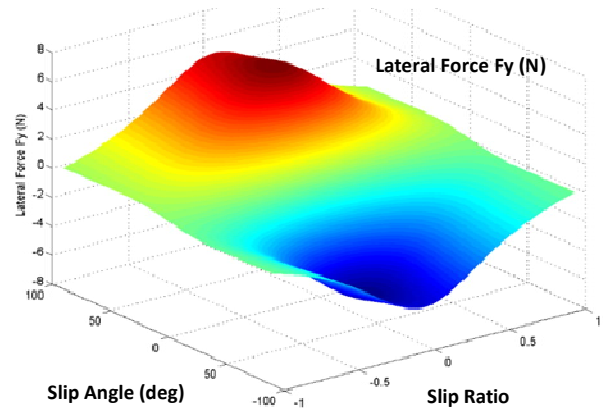


Fig. 12 Lateral force vs Slip condition

On the other hand, both Eqs. (4) and Eqs. (6) describe magnitude of longitudinal force, relating with slip ratio and slip angle respectively. The result of this estimation is shown in Fig. 13, where horizontal plane represents slip condition likewise Fig. 12. Except for the vertical axis, which represents longitudinal force, measured in Newton.

Longitudinal Force vs Slip Condition

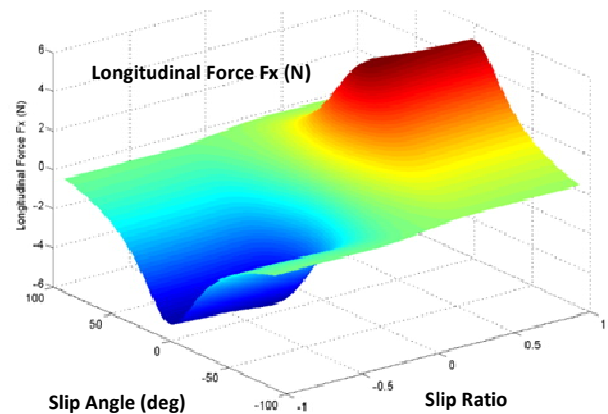


Fig. 13 Longitudinal force vs Slip condition

6. Comparison with Full Scaled Tire Model

The tire friction model of 1:10th scaled tire and that of full scaled tire [2, 9] were normalized by their vertical load to be friction coefficients so that estimating results of both models could be compared. The comparison between normalized 1:10th scaled tire model and full scaled tire model are illustrated in Fig. 14 – Fig. 17.

Consider the relationship plot of friction coefficient in Fig. 14 and Fig. 15, tire model of scaled tire similar to that of full size tire in many ways. First of all, force increases linearly with slip in the beginning, reaches maximum value. Eventually, the values slightly decrease until the full slip of each direction.

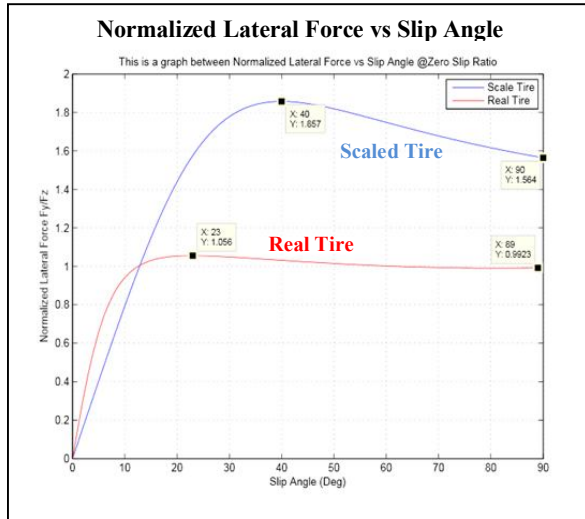


Fig. 14 Plot of Lateral force vs Slip angle Comparison with full scaled tire model

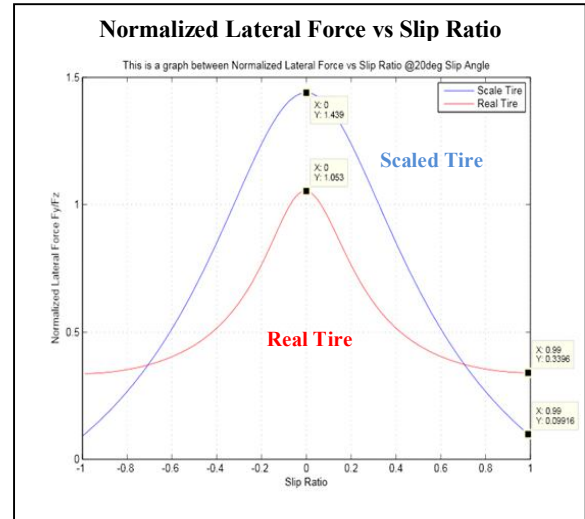


Fig. 16 Plot of Lateral force vs Slip ratio Comparison with full scaled tire model

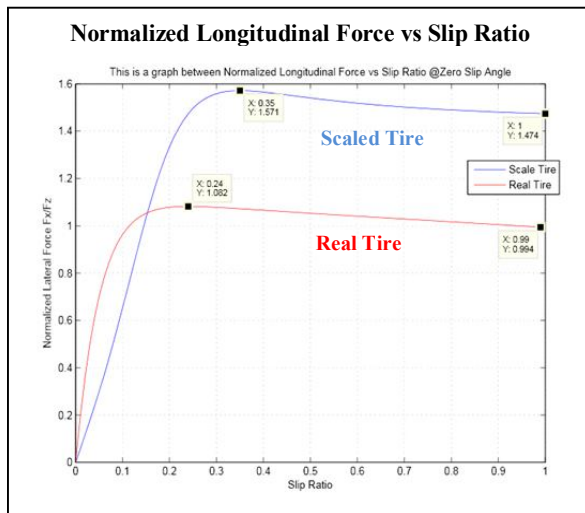


Fig. 15 Plot of Longitudinal force vs Slip ratio Comparison with full scaled tire model

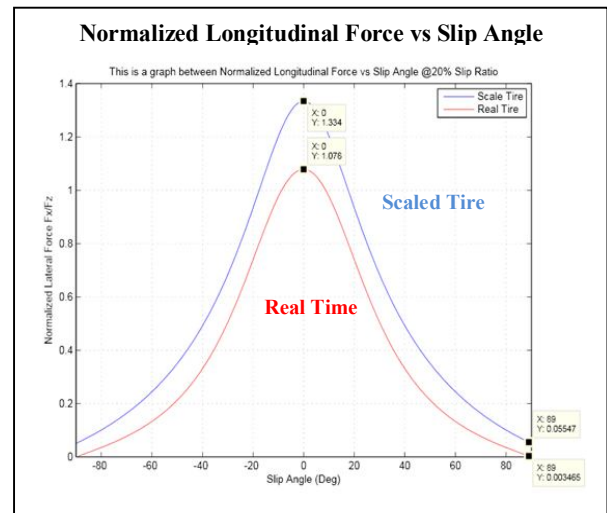


Fig. 17 Plot of Longitudinal force vs Slip angle Comparison with full scaled tire model

However, maximum force coefficients of scaled tire are significantly higher than that of full size tire; 80 percent in case of lateral force and 60 percent in case of longitudinal force. Moreover, the slip angle where maximum lateral force coefficients occur is larger, in case of scaled tire. Likewise, the slip angle where maximum longitudinal force coefficients occur is higher, in case of scaled tire.

Consider the relationship plot of friction coefficient in Fig. 16 and Fig. 17, tire model of scaled tire similar to that of full size tire in many ways. First of all, the maximum forces occur at zero slip, then the values decrease continuously until reach zero at full slip of each direction.

However, force coefficients of scaled tire are slightly higher than that of full size tire; 40 of maximum value in case of lateral force, likewise 25 percent in case of longitudinal force. Moreover, the tire force generated at full slip is slightly different as shown in the plots.

7. Discussion

According to the comparison between tire model of scaled tire and full size tire in the previous section, friction characteristic of scaled tire similar to that of full size tire in many ways. Therefore, it is possible to test on scaled vehicle; in order that, major dynamic characteristic of drifting phenomena on full size vehicle will be studied. However, the differences between tire force characteristics of scaled tire and full size tire should be reduced by two following ways.

The first way is to determine the suitable vertical load, affecting on friction coefficient. In the previous study, testing vertical load was determined by the actual load of HPI Pro D 1:10th scaled drifting car without supplementary load. In the future, the tested car must be modified consistent with Similarity law so that testing results on scaled vehicle test can be applied to real application. The additional weight loaded on tested car causes the increasing vertical load, affecting on characteristic of the scaled tire. For example, slip angle where maximum lateral force occurs will decrease.

Likewise, slip ratio where longitudinal force occurs will decrease. Eventually, friction characteristic of scaled tire will be more similar to that of full size tire.

The second way is to select the suitable type of scaled tire having desired and characteristic. There are many type of scaled tire, consisting different component. In the previous study, HPI T-Grip tires, 100 percent rubber, were used in the experiment. Because of their stickiness, scaled tire friction coefficients were higher than that of full size tire significantly. In the future, tested tire will have higher PVC ingredient in order to reduce scaled tire friction coefficient.

8. Conclusion

According to the experimental results obtained from drum tire test by the developed tire tester for 1:10th scaled tire, properties of scaled tire were studied. Friction characteristics of scaled tire similar to that of full size tire in many ways. The differences can be reduced by two suggested ways; to determine suitable vertical load consistent with Similarity law and to select scaled tires with suitable ingredient. Eventually, it is possible to explain drifting phenomena of real vehicle by testing on scaled vehicle, which is cheaper and safer.

9. Acknowledgement

This research was encouraged by Junior Science Talent Project (JSTP), the member of NSTDA.

10. References

- [1] Mujahid, A. (2006). On the Dynamics of Automobile Drifting, Society of Automotive Engineering, Inc., 20060-01-1019, 2006
- [2] Ronnapree, C. and Witaya, W. (2011). Two Dimensional Dynamic Model of Drifting Vehicle, paper presented in the 7th International Conference on Automotive Engineering, Bangkok, Thailand.
- [3] Ronnapree, C. and Witaya, W. (2011). Tire Test for drifting dynamic of a Scaled Vehicle, paper presented in the 8th International Conference on Automotive Engineering, Bangkok, Thailand.
- [4] Witaya, W., Parinya, W. and Krissada, C. (2008). Scaled Vehicle for Interactive Dynamic Simulation (SIS), paper presented in IEEE International Conference on Robotics and Biomimetics, Bangkok, Thailand.
- [5] Parinya, W., Wiwat, P. and Witaya, W. (2010). 3D Dynamic Model of A Real Scaled Vehicle, paper presented in the 6th International Conference on Automotive Engineering, Bangkok, Thailand.
- [6] Richard, T., O'Brien, Jr. and Jenelle, A. (2004). Scale Vehicle Analysis Using an Off-the-Shelf Scale-Model Testing Apparatus, paper presented in the 2004 American Control Conference, Massachusetts, USA.
- [7] Pacejka, H.B. (2002). *Tire and Vehicle Dynamics*, ISBN: 0768011264, SAE International.
- [8] Thomas, D.G. (1979). *Fundamentals of Vehicle Dynamics*, SAE International.
- [9] Tarunraj, S., *Tire Model in Driving Simulator*, Department of Mechanical and Aerospace Engineering, State University of New York at Buffalo, New York, USA, URL:<http://code.eng.buffalo.edu/dat/sites/tire/tire.html>, access on 22/02/2012
- [10] Rajeev, V. and Hosam, K.F. (2007), University of Michigan, *Development of a scaled vehicle with Longitudinal dynamics of a HMMWV for ITS test bed*, URL: <http://www.grad.chula.ac.th/download/thesis.pdf>, access on 22/11/2011.